

High Gain DC-DC Converter Based Hybrid Electric Vehicle (HEV) With Robust Integral Backstepping Control

Devika K A¹, Dr. Smitha B²

Student, EEE Dept., NSS College of Engineering, Palakkad, India¹

Professor, EEE Dept., NSS College of Engineering, Palakkad, India²

Abstract: High-gain, low voltage stress, small size, and high efficiency should be the defining characteristics of the DC-DC converter used in hybrid electric vehicles (HEV). This work suggests a new non-isolated DC-DC converter that uses switched capacitors and switched inductors to achieve high gain, a wide input voltage range, low voltage stresses across components, and a common ground topology. The electric vehicle using this converter under consideration employs a brand-new control method termed integral backstepping. The principle of the backstepping methodology described here is to decompose the system design problem into a series of lower order system subproblems, and then iteratively use the states discovered in the subproblems as virtual controls to derive the control law for the system.

Keywords: Electric Vehicle, Integral backstepping.

I. INTRODUCTION

Hybrid electric vehicles were developed in response to difficulties including the sharp decline in petroleum reserves, the scarcity of fossil fuels, environmental deterioration, and the escalating effects of global warming brought on by automobile emissions[4]. Therefore, the automotive sector must offer vehicles that are free of emissions and environmentally friendly[8]. The primary research topics that have drawn the attention of the transportation industry, researchers, and policy makers are the production of clean energy, its transmission, storage, utilisation, and energy management. Numerous vehicle designs, including plug-in hybrid electric vehicles (PHEVs), battery electric vehicles (BEVs), and fuel-cell electric vehicles (FHEVs), have been suggested to attain a greener transportation system.[5][6] Both PHEVs and BEVs need an external source, such as a charging station or the power grid, to ensure an uninterrupted supply of energy[7].

By adjusting the transformer turns ratio, an isolated DC-DC converter can quickly attain high-gain. But because of the transformer's leakage inductance, the circuit will generate a peak voltage that can easily damage the circuit's components. Leakage inductance can potentially affect the converter's efficiency and lead to issues with electromagnetic interference. The converter's size is further increased by the transformer in the isolated converter. The non-isolated DC-DC converter is more suited for HEVs when size, price, and efficiency are taken into account[2]. Since the mathematical models of HEVs are highly dynamic and nonlinear, nonlinear controllers may offer a better solution than their linear counterparts to account for the nonlinearities and parametric variations/uncertainties of the system [9]. Linear controllers only perform well in a small number of domains surrounding the reference point. A control algorithm based on variable structures has been presented for regulating the output voltage of HEVs powered by batteries and DC buses. For HEVs, a reliable backstepping controller has been proposed[3]. It does a decent job of tracking the DC bus voltage without providing any data on the vehicle's speed, but it does not account for the parametric changes of HEVs[1]. The output voltage regulation of HEVs has been proposed using an integral backstepping controller. It offers superior DC bus voltage tracking but is unable to provide data on the system's time-varying parametric values.

The hybrid energy storage system, power converters, and DC motor are the three key components of the unified model of the HEV[10]. Additionally, two energy sources—solar and battery—are the foundation of the Hybrid

Energy Storage System (HESS). The three important parts of HEV are hybrid energy storage system (HESS), power converters and DC motor[11].

II. HIGH GAIN DC-DC CONVERTER

In this work, a switched-capacitor and switched-inductor-based DC-DC converter is suggested. Fig. 1 depicts the suggested converter’s circuit topology. The input voltage is U_{in} , while the output voltage is U_o . The load resistance is R_L . Two power switches (Q_1 and Q_2), five diodes (D_1 through D_5), four capacitors (C_1 through C_4), and an inductor (L) make up the converter. The same gate drive signal S is used to simultaneously switch on and off Q_1 and Q_2 . $S=1$ and $S=0$ when power switches Q_1 and Q_2 are activated, respectively.

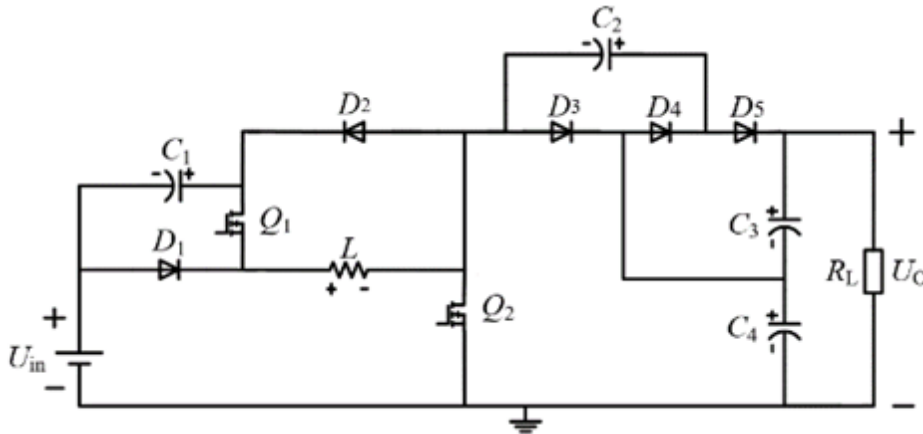


Fig. 1. Circuit diagram of high gain DC-DC converter

A. Operating Principle

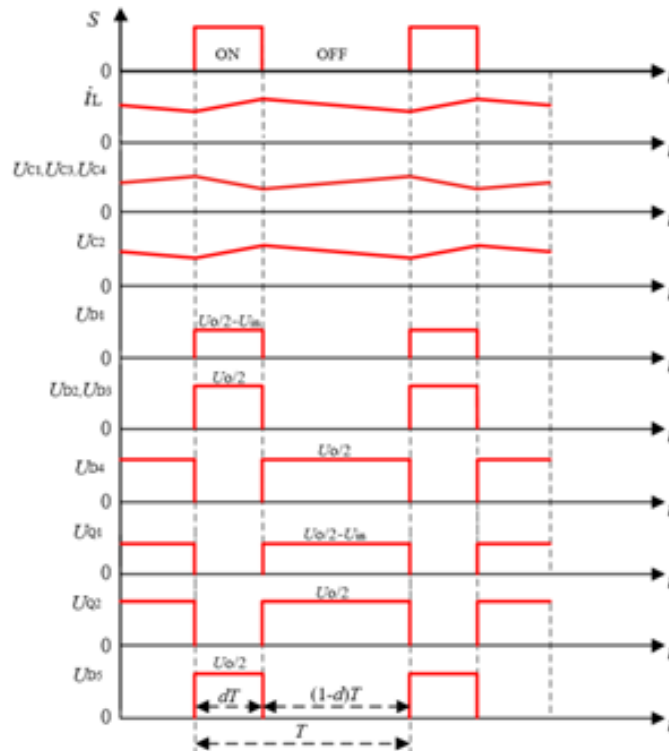


Fig. 2. Expected waveforms of proposed converter in CCM

The following assumptions are established in order to examine the suggested converter topology:

- 1) The power switch’s on-state resistance and the diode’s forward voltage drop are disregarded. Inductor and capacitor series resistances are equivalent and equal to 0.2.

2) The inductor is sufficiently large to guarantee that the circuit operates normally. The capacitors are big enough to guarantee that the capacitors' voltage ripple complies with the guidelines in this work.

When power switches Q_1 and Q_2 are turned on ($S=1$). Three current loops are visible in the circuit because the diodes D_1, D_2, D_3 and D_5 are reverse biased. Through Q_1 and Q_2 , the inductor L is charged by U_{in} and C_1 . Through the

power switch Q_2 and the diode D_4 , the capacitor C_4 charges the capacitor C_2 . Energy is transferred to the load R_L by the capacitors C_3 and C_4 's series components.

When power switches Q_1 and Q_2 are in the OFF state ($S=0$). There are four current loops in the circuit as a result of the diode D_4 being reverse biased. Capacitor C_1 is charged by inductor L through diodes D_1 and D_4 . Capacitor C_4 through D_1 and D_3 is charged by U_{in} and L . Through the diodes D_1 and D_5 , U_{in} , L , and C_2 charge the series portions of C_3 and C_4 . The capacitors C_3 and C_4 's series portion continues to supply energy to the load R_L .

B. Design Equations

The calculation equation of inductance can be obtained as

$$L = uL \frac{dt}{diL}$$

where f is the switching frequency of the converter and d is the duty cycle of the drive signal for power switches Q_1 and Q_2 . Assuming the current ripple of inductor L is ΔI_L , hence, the current ripple coefficient of inductor L is $\gamma = \Delta I_L / I_L$. In order to avoid excessive inductor current ripple, the ripple rate of inductor current is set as $\gamma \leq 0.4$.

The maximum inductor current and the maximum duty ratio can be obtained when the input voltage is the lowest. When the converter operates in the ON state, $u_L = u_{in} + u_{c1}$ and $dt = d \cdot T = d/f$. Final equation of inductance becomes,

$$L = \frac{d(1 - 2d)R_L}{4f\gamma}$$

The capacitance C can be calculated by,

$$C = i_c \frac{dt}{du_c}$$

C. Control Algorithm

A voltage boost type circuit with a set output voltage of 24V and an input voltage range of 9 to 15 volts was constructed. PWM signal is required since the circuit being constructed is a voltage converter that is controlled by PWM. Microprocessor PIC16f877A creates PWM signals. Additionally, the output voltage of the circuit will be applied to the analogue entrance of the PIC16f877A microcontroller since the output voltage of voltage boost type circuits must be at a constant 24V. By using the value obtained from the circuit's output, it is adjusted. Program will be written in MikroC PRO. The design of the power card and material selection are started after creating the control circuit and obtaining the proper PWM signal. This circuit topology will determine which components are required. The switching component will be a MOSFET transistor. The duty cycle is reduced until the desired output voltage is reached if the output voltage is larger than 24V. The duty cycle is increased until the desired output is reached if the output voltage is less than 24V. This code is repeatedly iterated by the CPU, which adjusts the output voltage in response to variations in the input voltage. The reference is verified once again after each loop to confirm the output voltage is maintained.

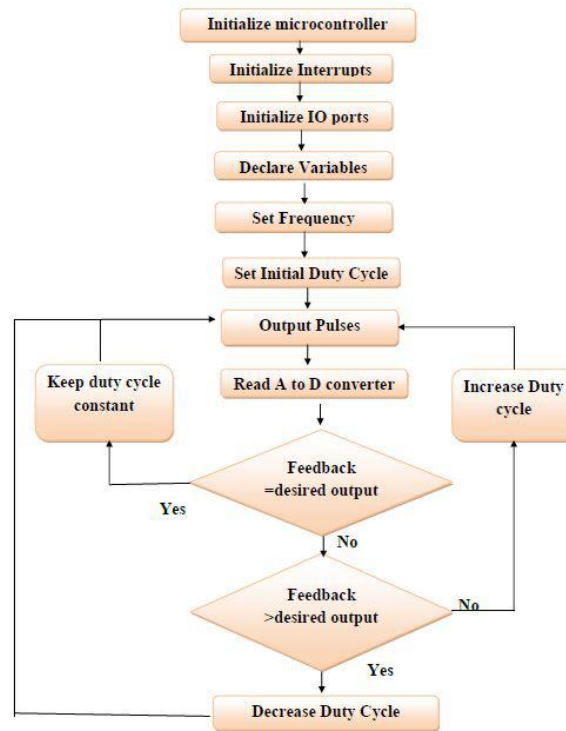


Fig. 3. Control Algorithm of DC-DC Converter

D. Comparison with other Converters

The proposed converter is compared with other converters in terms of voltage gain, voltage stress, the number of components, and common ground structure, as shown in Table 1. Compared with conventional boost converter, the proposed converter can obtain a higher gain. When the proposed converter achieves high-gain, the duty cycle is always less than 0.5 without extreme duty cycle. Furthermore, the voltage stresses across components of the proposed converter are no more than $U_0/2$, rather than the $U_0/2$ of conventional boost converter. The low voltage-stress can reduce the volume and cost of the capacitors, which occupy large volume of converter. The low voltage-stress can also reduce the voltage breakdown risk of the device and improve the reliability of the converter.

Converters	Voltage gain	Inductors	Capacitors	Power switches	Diodes	Voltage stresses across capacitors	Voltage stresses across diodes	Voltage stresses across power switch	Common ground structure
Boost converter	$1/(1-d)$	1	1	1	1	U_0	U_0	U_0	Yes
Input-ParallelOutput-Series DC-DC Boost Converter With a Wide Input Voltage Range	$2/(1-d)$	2	3	2	3	$U_0/2$	$U_0/2$	$U_0/2$	No
Single-Switch, Wide Voltage-Gain Range, Boost DC-DC Converter	$2/(1-d)$	1	3	1	3	$U_0/2$	$U_0/2$	$U_0/2$	No
Wide Input-Voltage Range Boost Three-Level DC-DC Converter With Quasi-Z Source	$2/(3-4d)$	2	4	3	4	$\leq U_0/2$	$U_0/2$	$U_0/2$	Yes
Quasi-Z-converter	$1/(1-2d)$	2	3	1	2	U_0	U_0	U_0	Yes
Z-source DC-DC converter with cascade switched capacitor	$(1+d)/(1-2d)$	3	5	1	3	$U_0/(1+d)$	$U_0/(1+d)$	$U_0/(1+d)$	No
Proposed converter	$2(1-d)/(1-2d)$	1	4	2	5	$\leq U_0/2$	$\leq U_0/2$	$\leq U_0/2$	Yes

Table 1- Comparison of various Converters

III. CONTROL OF MOTOR

A high voltage, high current dual full-bridge motor driver IC called L298N is used to manage stepper and DC motors. Two DC motors can have their rotation, speed, and direction controlled. An L298 dual-channel H-Bridge motor driver IC makes up this driver. It employs two methods to regulate the DC motors' rotational direction and speed. These are H-Bridge for regulating rotational direction and PWM for managing speed. These modules have simultaneous control over two DC motors or one stepper motor. Two methods are used in this driver to regulate the DC motors' rotational direction and speed. These include H-Bridge, which controls rotational direction, and PWM, which controls speed.

IV. INTEGRAL BACKSTEPPING CONTROL METHODOLOGY

Integral with extensions to MISO (multiple-input, single-output) systems in component form, backstepping control is primarily focused on adaptive and nonlinear management of SISO (single-input, single-output) systems. The fundamental principle of the backstepping methodology is to decompose the system design problem into a series of lower order subproblems, and then iteratively use the states discovered in the subproblems as virtual controls to discover the control law of the system. The Control Lyapunov Function is used to determine the subproblem transitional control rules. The back-stepping control ensures that regional subsystems are stable on a global scale, prevents non-linearity cancellation, and does not call for differentiators.

In this project, the model of a DC motor was developed, and the tracking control was carried out using the backstepping control methods. Making a DC motor system's output follow a reference or desired trajectory was the study's objective. By putting the methods outlined in the following paragraphs into practise, a direct relationship between the output and input of the DC motor was obtained with the aid of the backstepping control approach algorithm.

The position error tracking was chosen as the initial regulated variable, and the velocity was chosen as the control variable first. This was the DC motor system's initial subsystem. The first subsystem control law was obtained using the Control Lyapunov Function. The velocity error tracking signal was chosen as the second regulated variable, and the torque/current was chosen as the control variable. This developed into the DC motor system's second subsystem. The first subsystem error tracking signal is part of the second subsystem's Control Lyapunov Function. The control law of the second subsystem was accomplished with the aid of the Lyapunov function.

Finally, a third error signal was chosen in order to make a connection between the input and the output. We looked for a control law that will asymptotically stabilise the DC motor system using the Control Lyapunov Function. The error signals converged to zero and the position and velocity of the DC motor system converged to the reference/desired signals as a result of asymptotically stabilising the system. Following the correct implementation of the backstepping control mechanism, more investigation of the system response was carried out in MATLAB to enhance the total DC motor output tracking of a reference/desired trajectory.

The input control u is asymptotically stabilizing the system and are negative definite, the closed loop system is asymptotically stable and the error variables z_1, z_2 and z_3 converge to zero. As a result, the angular rotor position θ and the rotor angular velocity w converge to the reference position and respectively the reference velocity.

$$u = J(-k_1 z_1 - K\sigma + z_2)(1 + k_1 k_2) + x_2 \left[(k_1 + k_2)k_f + \frac{(k_f')^2}{J} - \frac{(k_e)}{L} \right] - x_3 \left[(k_1 + k_2)k_t - \frac{R}{L} + \frac{k_f k_t}{J} \right] + J(k_1 + k_2)T_L + J\ddot{x}_1 - \dot{T}_L + k_3 z_3 - Kz_1 + J(k_1 + k_2)$$

V. SIMULATION AND RESULTS

The full hybrid electric vehicle (HEV) system discussed in this project work is simulated in Matlab. Solar PV panels, batteries, and an external charging connection are the energy sources employed. A DC motor is connected to the converter's output, which is coupled to the boost DC-DC converter that is being used. 12V is the input voltage that is used. The state of charge (SOC) of the battery, the output voltage and current of the solar PV panel, the input and output voltage of the high gain DC-DC converter, and ultimately the motor output speed are all results from this simulation.

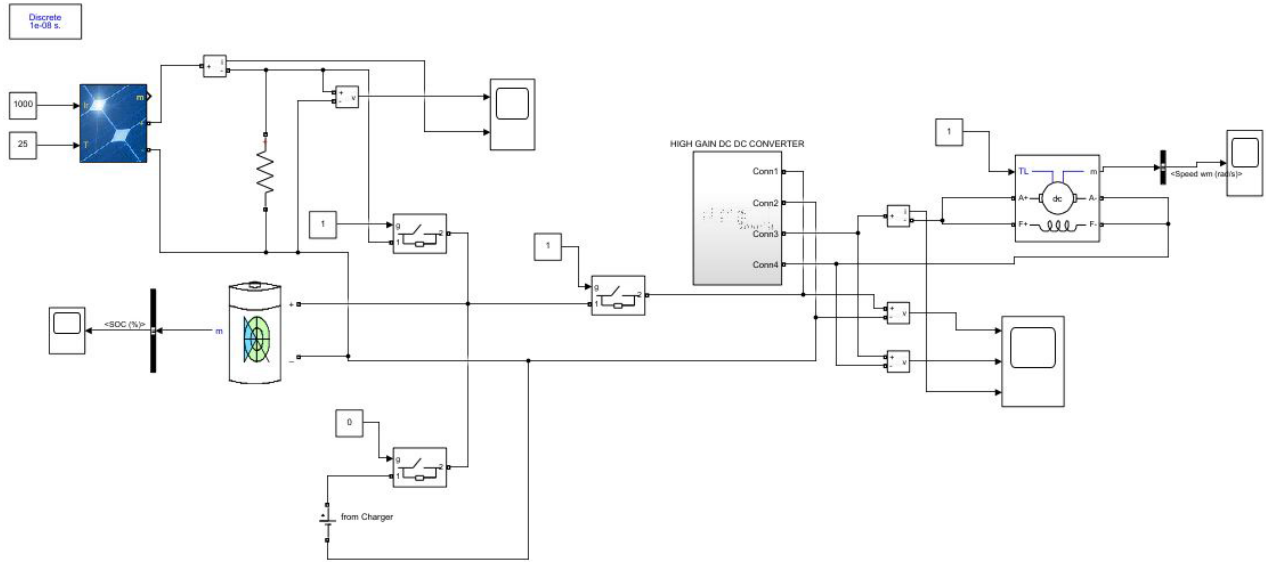


Fig. 4. Simulation diagram of HEV system

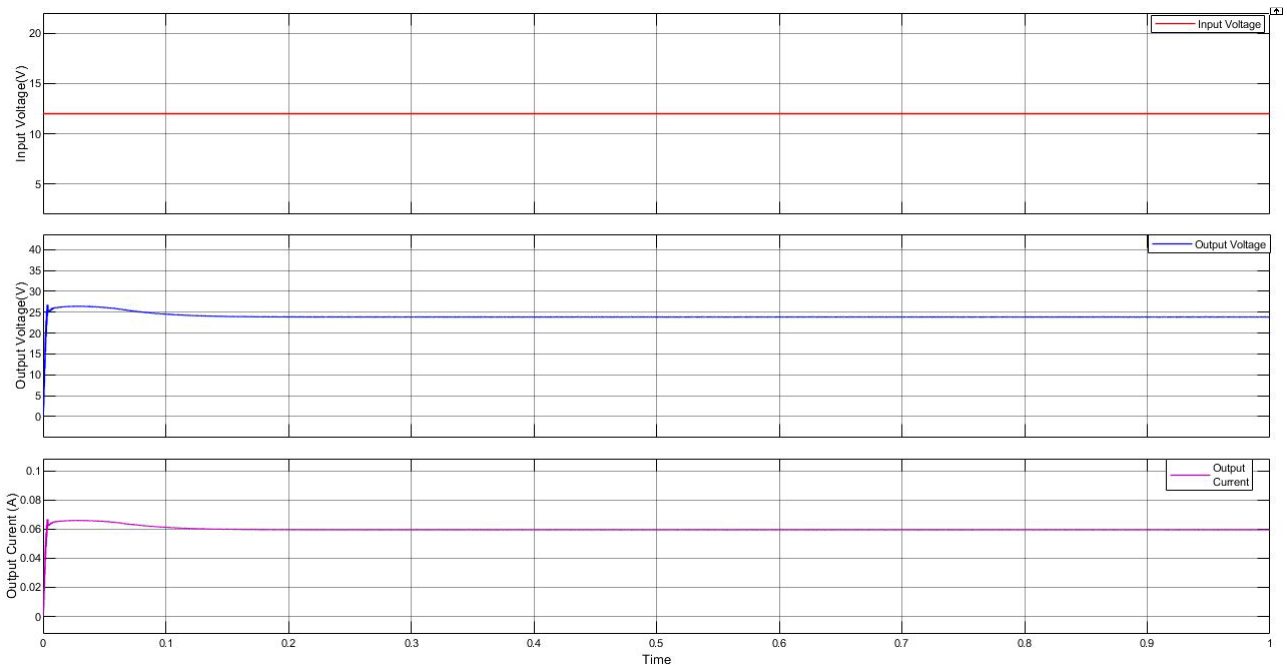


Fig. 5. High gain DC-DC Converter output

To confirm the stability and asymptotic tracking performance of the integral backstepping design, simulation is done in MATLAB/Simulink. To assess the position and velocity tracking as well as the stability of the design, an independently excited DC motor model was first employed as a reference/desired input to the system. Second, the performance of the integrated backstepping design's velocity and position tracking was assessed using a sinusoidal input as the rotor reference/desired velocity.

The DC Motor's angular velocity response has an overshoot, which contributes to some mistake in the tracking of angular location. Either the DC motor parameter selection or the control law Simulink implementation was the source of the overshoot. Nevertheless, by using the computed control law equation in Simulink, the tracking of the reference velocity signal has been accomplished.

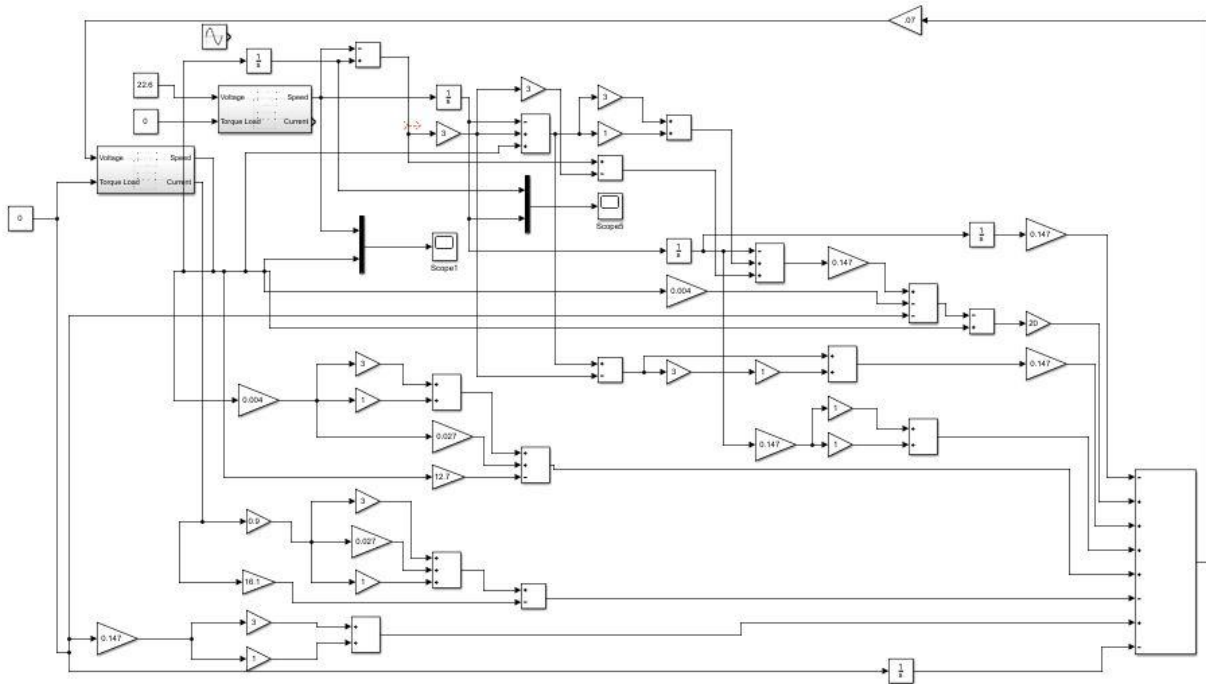


Fig. 6. DC motor Simulink of integral backstepping control

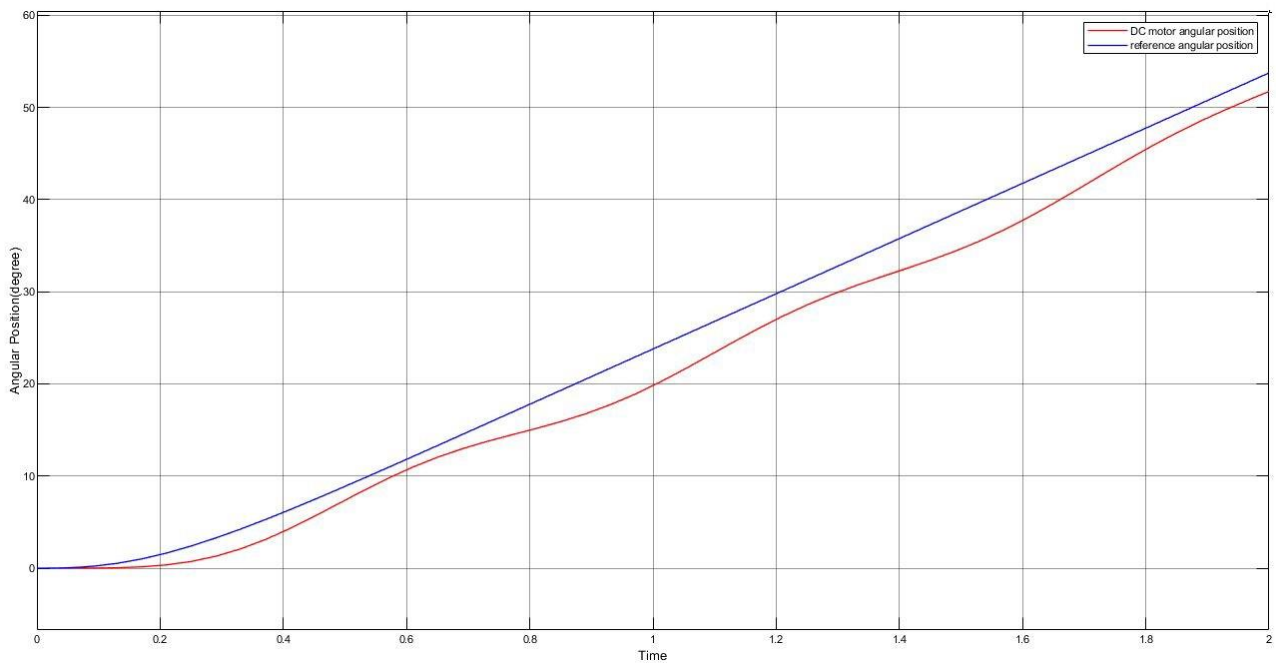


Fig. 7. DC Motor angular position tracking

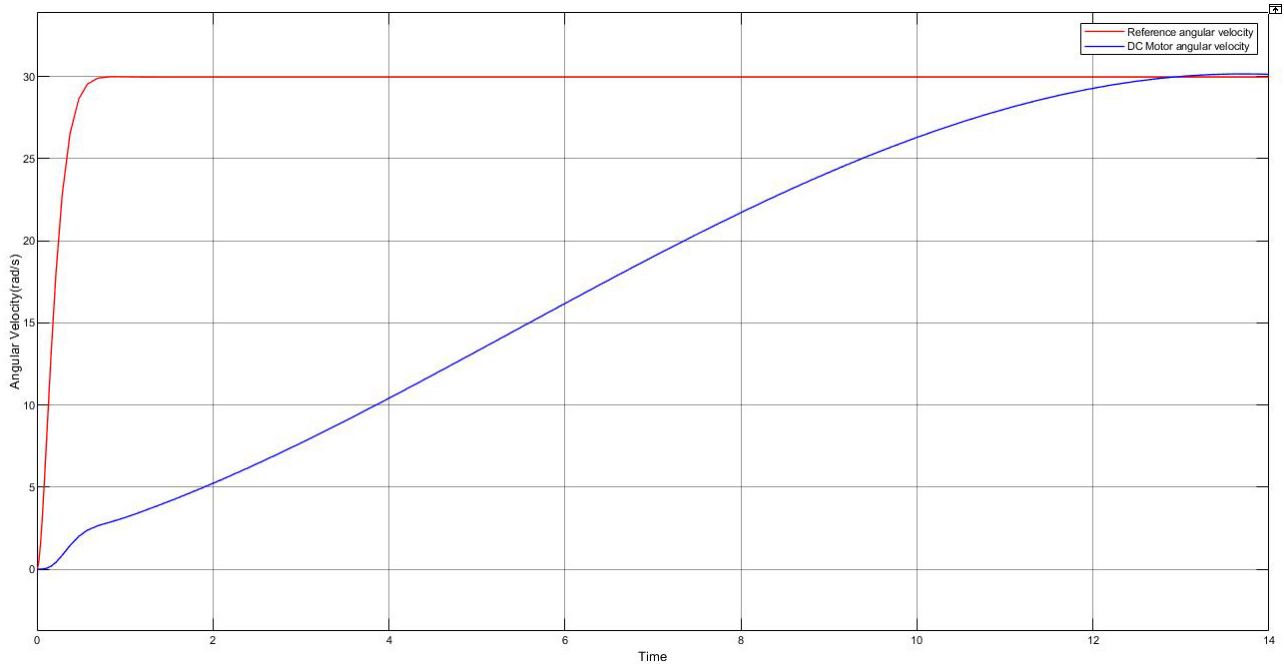


Fig. 8. DC Motor angular velocity tracking

VI. **HARDWARE IMPLEMENTATION**

Solar PV panels, batteries, or an external power source can all be used to generate the 12V input voltage. Battery charging options include using an external power source or a solar PV panel. The DC motor, which propels the hybrid electric vehicle (HEV), receives its output from the DC-DC converter after receiving power from the battery.



Fig. 9. Hardware setup of proposed system

VII. CONCLUSION

This research work includes a unified model of a hybrid electric vehicle, a high gain DC/DC converter, and introduces robust integral backstepping for motor speed control and DC bus voltage management. For hybrid automobiles, this project provides a non-isolated DC-DC converter topology. It is advantageous to lower the size and price of the converter since the voltage stresses across components are less than half of the output voltage. The control system has been implemented using a PIC 16F877a microcontroller. MATLAB is used to simulate a DC/DC converter and implement it in an experimental testing environment. The results of the simulation and the testing demonstrate that the suggested high gain DC-DC converter can generate a constant output voltage of 24V. By using closed loop control, the converter can always keep the output voltage stable for an uncontrolled input voltage. The converter that is being proposed is appropriate for hybrid electric vehicles.

To regulate the angular velocity and angular position tracking of a DC Motor system in a hybrid electric vehicle, the integral backstepping design was used. By applying the Lyapunov and backstepping theories, a control law was calculated. According to the backstepping design theory, the error signals (velocity and position) must converge to zero in order for the calculated control law to be assured of being asymptotically stable. The adaptive rules have been used to estimate the system's unknown time-varying properties.

REFERENCES

- [1] Muhammad Muzammal Islam, Syed Ahmad Siffat, Iftikhar Ahmad, Muwahida Liaquat, Safdar Abbas Khan, "Adaptive Nonlinear Control of Unified Model of Fuel Cell, Battery, Ultracapacitor and Induction Motor Based Hybrid Electric Vehicles", IEEE Access Year: 2021, Volume: 9, Journal Article, Publisher: IEEE
- [2] Xiaogang Wu, Mingliang Yang, Meilan Zhou, Yu Zhang Jun Fu, "A Novel High-Gain DC-DC Converter Applied in Fuel Cell Vehicles" IEEE Transactions on Vehicular Technology, Year: 2020, Volume: 69, Issue: 11, Journal Article, Publisher: IEEE
- [3] Syed Ahmad Siffat, Iftikhar Ahmad, Aqeel Ur Rahman, And Yasir Islam, "Robust Integral Backstepping Control for Unified Model of Hybrid Electric Vehicles", IEEE Access, Year: 2020, Volume: 8, Journal Article, Publisher: IEEE
- [4] S. Shaei and R. A. Salim, "Non-renewable and renewable energy consumption and CO2 emissions in OECD countries: A comparative analysis," Energy Policy, vol. 66, pp. 547556, Mar. 2014.
- [5] H. E. Dance, "The electric battery vehicle," J. Inst. Electr. Eng., vol. 61, no. 323, pp. 110041108, Oct. 1923.
- [6] F. A. Wyczalek, "Hybrid electric vehicles: Year 2000 status," IEEE Aerosp. Electron. Syst. Mag., vol. 16, no. 3, pp. 1525, Mar. 2001.
- [7] S. Hardman, E. Shiu, and R. Steinberger-Wilckens, "Changing the fate of fuel cell vehicles: Can lessons be learnt from tesla motors?" Int. J. Hydrogen Energy, vol. 40, no. 4, pp. 16251638, Jan. 2015.
- [8] Z. Dimitrova and F. Mar'echal, "Technoeconomic design of hybrid electric vehicles and possibilities of the multi-objective optimization structure," Appl. Energy, vol. 161, pp. 746759, Jan. 2016.
- [9] N. van deWouw, E. Lefeber, and I. L. Arteaga, Nonlinear Systems. Cham, Switzerland: Springer, 2017, doi: 10.1007/978-3-319-30357-4.
- [10] H. Armghan, I. Ahmad, N. Ali, M. F. Munir, S. Khan, and A. Armghan, "Nonlinear controller analysis of fuel cell battery ultracapacitor-based hybrid energy storage systems in electric vehicles," Arabian J. Sci. Eng., vol. 43, no. 6, pp. 31233133, Jun. 2018, doi: 10.1007/s13369-018-3137-y.
- [11] H. El Fadil, F. Giri, J. M. Guerrero, and A. Tahri, "Modeling and nonlinear control of a fuel cell/supercapacitor hybrid energy storage system for electric vehicles," IEEE Trans. Veh. Technol., vol. 63, no. 7, pp. 30113018, Sep. 2014.